First-principles study of oxygen vacancies in Lu_2SiO_5

2007 J. Phys.: Condens. Matter 19 436215

(http://iopscience.iop.org/0953-8984/19/43/436215)

IOP PUBLISHING JOURNAL OF PHYSICS: CONDENSED MATTER

J. Phys.: Condens. Matter **19** (2007) 436215 (8pp) doi:10.1088/0953-8984/19/43/436215

First-principles study of oxygen vacancies in Lu_2SiO_5

Bo Liu[1], **Zeming Qi**[2], **Mu Gu**[1], **Xiaolin Liu**[1], **Shiming Huang**[1] **and Chen Ni**[1]

[1] Laboratory of Waves and Microstructure Materials, Pohl Institute of Solid State Physics, Tongji University, Shanghai 200092, People's Republic of China
[2] National Synchrotron Radiation Laboratory, University of Science and Technology of China, Hefei 230027, People's Republic of China

Received 18 April 2007, in final form 11 September 2007
Published 28 September 2007
Online at stacks.iop.org/JPhysCM/19/436215

Abstract

We investigated the oxygen vacancies in Lu_2SiO_5 (LSO:Ce) by using first-principles pseudopotential calculations based on density functional theory. The results indicate that V_{O5} has the lowest formation energies compared with the other four oxygen vacancies belonging to the SiO_4 tetrahedron. The oxygen vacancy can induce extra states in the band gap. The 2+ charge state vacancies are energetically favorable and show lower formation energies with respect to the neutral vacancies. V_{O5} could act as electron trap which could be responsible for the afterglow emission for LSO:Ce.

1. Introduction

Ce doped Lu_2SiO_5 (LSO:Ce) is being extensively studied [1–6] because of its high light yield of about 30 000 photons MeV^{-1}, high density of 7.4 g cm^{-3}, short scintillation decay time of several tens of ns and energy resolution of 9.0% FWHM for the ^{137}Cs γ-source full energy peak as well as high time resolution of 450 ps. This material is a promising medical scintillator for applications in positron emission tomography (PET) imaging systems which can follow the body's physiological functions, such as blood flow and metabolism [7]. The scintillator light is due to the parity-allowed electric dipole 5d $\rightarrow$ 4f transition of the Ce^{3+} ion which is strongly affected by the crystal field. It is established that the Ce^{3+} luminescence in the LSO host exhibits excitation and emission spectra of two distinct types under ultraviolet excitation, with contributions from two luminescent centers Ce1 and Ce2. Our previous studies show that energy transfer from Ce1 center to Ce2 center can occur and can be enhanced by the rising temperature [8].

Although LSO:Ce crystals show excellent scintillation performance, they also exhibit a rather strong afterglow, which is a negative property and should be eliminated as far as possible. Very strong thermoluminescence curves above room temperature were reported by many studies [9–11]. It is suggested that oxygen vacancies may be related to the trap centers in LSO.

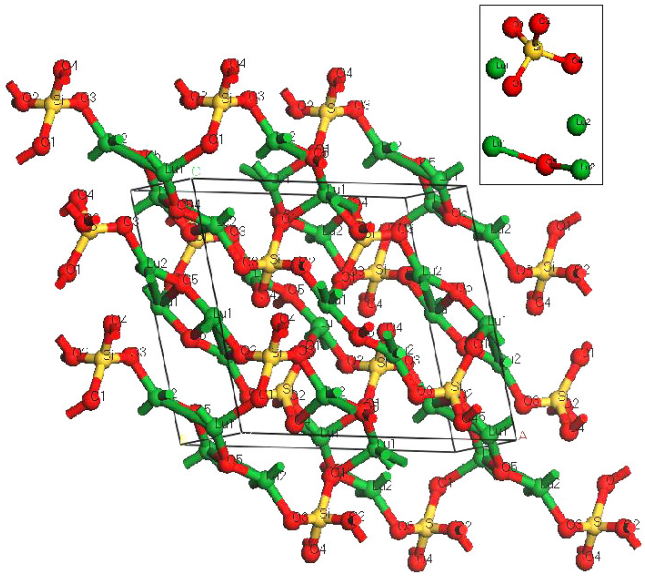

Figure 1. The structure of the unit cell of LSO and the schematic view of the tetrahedral SiO_4 and Lu–O chain in the LSO cell in the inset.

(This figure is in colour only in the electronic version)

LSO has a monoclinic structure with the space group of $C2/c$. In the structure of LSO, shown in figure 1, there exists a SiO_4 tetrahedron with oxygen sites of four different types (O1–O4) and one type of non-silicon-bonded oxygen atom (O5) surrounded by four Lu atoms [12]. The Lu ions occupy two crystallographically independent sites with oxygen coordination numbers of 6 and 7. Since oxygen vacancies may play a critical role for the defects in LSO, it is necessary to investigate the oxygen vacancies using theoretical calculations.

In this paper, we use a first-principles pseudopotential method to calculate the formation energies of the oxygen vacancies, levels of transition between the different charged oxygen vacancies, and the density of states for the perfect and the oxygen vacancy-containing LSO. A possible model for oxygen vacancies behaving as trap centers is also discussed.

2. Method of calculations

Density functional theory (DFT) Calculations within the local-density approximation (LDA) in the Teter–Padé parameterization [13] were performed using plane-wave pseudopotential code ABINIT [14][3]. Norm-conserving Troullier–Martins [15] type pseudopotentials for Lu, Si and O were used. The electronic wavefunctions were expanded in plane waves up to a kinetic energy cut-off of 50 Ha (1 Ha $=$ 27.211 eV), and it was confirmed that the total energies were converged within 1 meV/atom for the total energies obtained at 60 Ha. A unit cell has eight LSO molecules and 64 atoms. We optimized the lattice constant of the unit cell with the experimental data ($a = 14.277$ Å, $b = 6.639$ Å and $c = 10.224$ Å) as initial input. The calculated result ($a = 14.025$ Å, $b = 6.583$ Å and $c = 10.116$ Å) is highly consistent with the experimental one. Brillouin zone integrations were made with a $2 \times 2 \times 2$ k-point mesh

[3] The ABINIT code is a project in common of the Université Catholique de Louvain, Corning Incorporated, and other contributors.

generated according to the Monkhorst–Pack scheme [16]. An oxygen atom is removed from the perfect crystal to simulate the oxygen vacancy. The neutral defect is defined as the system in which an oxygen atom is removed and two electrons are left behind at the vacancy. The charge state can be changed up to $Q = 2+$. The $Q = 2+$ charge state of the oxygen vacancy corresponds to a removal of a doubly negatively charged oxygen anion from the perfect crystal. The five oxygen atoms in LSO are labeled as O1–O5, as shown in figure 1.

The optimized geometry of the neutral system was used as the initial structure for the corresponding charged system. All the atoms were allowed to relax using the Broyden–Fletcher–Goldfarb–Shanno (BFGS) [17] algorithm until the maximum residual force was less than 5 meV Å^{-1}.

The formation energy $\Delta H_f(\alpha, q)$ of an oxygen vacancy in charge state q is a function of both the electron chemical potential μ_e and the oxygen chemical potential μ_O [18]:

$$\Delta H_f(\alpha, q) = E(\alpha, q) - E(\text{perfect}) + \mu_O^0 + \mu_O + q(E_F + E_{VBM}) \tag{1}$$

where $E(\alpha, q)$ is the total energy of the cell containing an oxygen vacancy in a charge state q which is 0, 1+ or 2+ for V_O, V_O^+ and V_O^{2+}, respectively. E (*perfect*) is the total energy of the perfect cell. For the studies of charged defects, an electron or two electrons are removed from the neutral system and a uniform background with opposite polarity is adopted automatically to maintain the neutrality of the whole system, so the total energy per cell does not become infinite. The μ_O is the oxygen chemical potential with respect to energy of molecular oxygen μ_O^0. The μ_O^0 was obtained from the calculated total energy of an O_2 molecule in a cubic box of $15 \times 15 \times 15$ Å^3. E_{VBM} is the energy of the valence band maximum which should be determined for the formation energy of the charge state defect. In order to determine E_{VBM} for the defective cell, the band structures of the perfect and defective cell must be lined up [19]. E_F is the Fermi energy of the electrons referenced to the valence band maximum of LSO.

The defect transition energy level $\varepsilon_\alpha(q/q')$ is defined as the value of the Fermi level where the formation energy of q is equal to that of another charge q' of the same defect, i.e. [20]

$$\varepsilon_\alpha(q/q') = [\Delta E(\alpha, q) - \Delta E(\alpha, q')]/(q' - q). \tag{2}$$

The chemical potentials are restricted by the following equilibrium conditions:

$$2\mu_{Lu} + \mu_{Si} + 5\mu_O = \Delta H_f(Lu_2SiO_5) \tag{3}$$

is the equilibrium condition for formation of Lu_2SiO_5.

$$2\mu_{Lu} + 3\mu_O \leqslant \Delta H_f(Lu_2O_3) \tag{4}$$

$$\mu_{Si} + 2\mu_O \leqslant \Delta H_f(SiO_2) \tag{5}$$

are required to prevent the formation of Lu_2O_3 and SiO_2, respectively.

$$\mu_{Lu} \leqslant 0, \qquad \mu_{Si} \leqslant 0, \qquad \mu_O \leqslant 0 \tag{6}$$

are also needed to prevent precipitation of elemental solid Lu, Si and molecular (O_2), respectively.

Here, ΔH_f is the generalized formation free energy of the corresponding solid compound relative to bulk Lu, Si and molecular oxygen. From the above limit, we determine the oxygen chemical potential $\mu_O = -5.3$ eV for the oxygen-poor limit which is close to the LSO crystal growth conditions.

The densities of states for perfect and defective cells are calculated with a Gaussian smearing of 0.01 Ha. The Brillouin zone integrations were made with a $2 \times 2 \times 2$ k-point sampling generated according to the Monkhorst–Pack scheme for the DOS calculations.

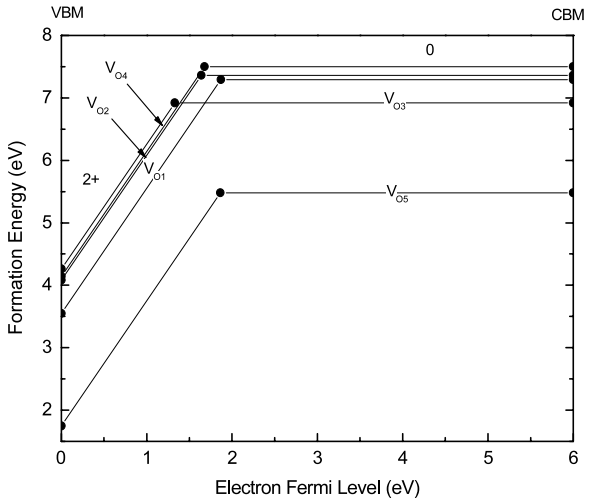

Figure 2. Formation energies as a function of the electron Fermi energy E_F. Only the lowest energy charge states with respect to E_F are shown. The charge state determines the slope of each line segment. Only the charge state that gives the lowest formation energy with respect to the Fermi level is depicted.

3. Results and discussion

The calculated formation energies for the five oxygen vacancy types as a function of electron Fermi energy are shown in figure 2. Only the charge state that gives the lowest formation energy with respect to the Fermi level is depicted. Since there is negative-U behavior for oxygen vacancies, which will be discussed below, the V_O^+ defects show higher energies than those of V_O or V_O^{2+} for the whole Fermi level, and thus are not shown in figure 2. The formation energies for oxygen vacancies are also listed in table 1 including neutral, 1+, and 2+ charge states for the five oxygen vacancy types. The formation energies for charge states are given for the Fermi level set at the valence band maximum (VBM).

The formation energies for neutral V_{O1}–V_{O5} are rather high, indicating that they are unlikely to form even at high temperature during growth. However, at charge states, their formation energies are obviously lower. V_{O5} has the lowest formation energy for both neutral (6.98 eV) and 2+ charge states (1.75 eV) compared with the other four oxygen vacancies. The low formation energy means that V_{O5} is the dominant oxygen vacancy. It is worthwhile noting that, during H^+ irradiation, the oxygen vacancies are increased further [21]. In such a situation, which is a non-equilibrium condition, even oxygen vacancies with high formation energies can form under irradiation.

For the cases of V_{O1} to V_{O4}, the silicon atom moves slightly towards the missing oxygen in its tetrahedron. The remaining Si–O bond lengths are increased by about 3%. In the charged defect V_O^+, the Si atom moves back towards its initial position. For V_O^{2+}, the distance between the Si and oxygen vacancy are further increased, as shown in table 2. The distance is calculated using the coordinate of the oxygen vacancy where the oxygen atom is removed and the coordinate of the relaxed Si atom. Since the SiO_4 tetrahedron is rather stable, breaking the Si–O bond requires relatively high energy. The fifth type of oxygen is surrounded by Lu atoms, showing the strong ionic character rather than covalent character of the Si–O bond. The calculated formation energy of the V_{O5} is much lower than those of V_{O1}–V_{O4} at neutral or charge states. One may understand this result by considering the different bonds for the

Table 1. Formation energies for oxygen vacancies and transition energy levels. The energies are given in eV. The formation energies for charge states are given for the Fermi level set at the VBM.

Defects	Neutral (VO)	1+ charge state (V_O^+)	2+ charge state (V_O^{2+})	Energy level of transition between neutral and 2+ charge state
V_{O1}	7.29	5.62	3.55	$E_v + 1.47$
V_{O2}	7.36	5.96	4.08	$E_v + 1.24$
V_{O3}	6.92	5.85	4.26	$E_v + 0.93$
V_{O4}	7.50	5.99	4.14	$E_v + 1.28$
V_{O5}	5.48	3.84	1.75	$E_v + 1.46$

Table 2. The distances between Si and the oxygen vacancy in the SiO_4 tetrahedron. Superscripts stand for charge states. The distances in the unrelaxed configuration are also shown in a column. Units: Å.

Parameter	Unrelaxed V_O	V_O	V_O^+	V_O^{2+}
V_{O1}	1.74	1.46	1.67	2.18
V_{O2}	1.64	1.35	1.57	2.08
V_{O3}	1.59	1.32	1.54	1.99
V_{O4}	1.72	1.44	1.62	2.12

Table 3. The distances between Lu1 and Lu2 and the fifth oxygen vacancy V_{O5}. Superscripts stand for charge states. The distances in the unrelaxed configuration are also shown in a column. Units: Å.

Parameter	Unrelaxed V_O	V_O	V_O^+	V_O^{2+}
Lu1–O5	2.36	1.80	2.42	2.61
Lu2–O5	2.41	2.16	2.46	2.59

different oxygens. The energy for breaking the Si–O bond is higher than that for the Coulomb interaction of Lu–O. Additionally, O5 locates in a relatively large space. The shortest Lu–O5 distance is about 2.16 Å and the O5–O5 distance is 2.91 Å. The large space for the O5 atom makes the interaction with other atoms weak and leads to a low vacancy formation energy. The distances for the Lu and oxygen vacancy are shown in table 3. When the O5 is removed from the perfect cell, forming a neutral oxygen vacancy, the neighboring Lu1 and Lu2 atoms relax towards the vacancy. For the positively charged states of V_{O5}^+ and V_{O5}^{2+}, the Lu1 and Lu2 relax backwards to the vacancy due to the electrostatic repulsion between Lu and the positively charged vacancy. In addition, for the V_{O5}, the distance between Lu1 and Lu2 is 2.70, 3.47 and 3.64 Å for the neutral, 1+ and 2+ states of the oxygen vacancy, respectively, while the distance in the perfect crystal is 3.39 Å. For comparison, the distance between Lu atoms in the hexagonal-close-packed (hcp) Lu metal is 3.43 Å. Therefore, in the case of neutral V_{O5}, chemical re-bonding between the Lu1 and Lu2 ions is possible due to the short distance, which can also lower the total energy of the system. This can partly explain why V_{O5} has lower formation energies than other oxygen vacancies.

From the present calculations, there is a negative-U behavior [22] for the five oxygen vacancies. This means that only neutral and 2+ charge state vacancies are stable, while the 1+ charge state is never stable in equilibrium conditions. The formation energies of V_O^+ are higher than those of V_O or V_O^{2+} at all values of E_F.

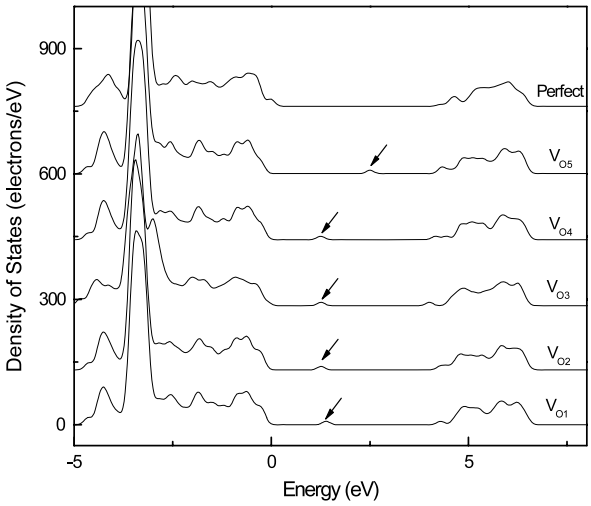

Figure 3. Density of states for the perfect LSO and V_O-containing LSO. The valence band maximum for perfect LSO is set at 0 eV. The highest occupied levels for the V_O-containing LSO are denoted by arrows.

The negative-U energy is defined by

$$U = \varepsilon(+/0) - \varepsilon(2+/+) = \Delta H_f(V_O^{2+}) + \Delta H_f E(V_O) - 2\Delta H_f(V_O^{+}). \quad (7)$$

The U values are in the range of -0.3 to -0.5 eV. The negative-U behavior can be interpreted in terms of the large relaxation when the V_O^+ lose an electron becoming V_O^{2+}, which lowers the energy of V_O^{2+}. However, it should be noted that the periodic boundary condition may lead to error due to the electrostatic energy for the array of charged vacancies, since a finite-size cell is used in the calculations [23]. The boundary effect is larger for the $2+$ charge state than the $1+$ charge state. Therefore, the negative U may be reversed and an artifact of the computational approach. In addition, the equilibrium concentration of defects will change since the formation energies will increase due to the electrostatic contribution.

The density of states (DOS) for the perfect LSO and V_O-containing LSO are shown in figure 3. The band gap shown in the DOS is underestimated compared with the experimental value (6 eV) [8], which is a commonly observed feature for LDA calculation. In figure 2, the band gap is adjusted to match the experiment value by moving the conduction band up. The valence band maximum for perfect LSO is set at 0 eV. For perfect LSO, the top of the valence band mainly originates from the O 2p states, below which Si 3p states and Lu 4f states are mainly located at -7 to -5 eV. The conduction band is mainly comprised of Lu 5d states. As can be seen from figure 3, the overall DOS profiles for the V_O-containing LSO are quite similar to those of the perfect LSO. However, the oxygen vacancy may induce extra states in the band gap, which are denoted by arrows in figure 3. The induced defect states are located at 1.38, 1.24, 1.25, 1.25, and 2.50 eV above valence band maxima for V_{O1} to V_{O5}, respectively. Integration of the DOS in the energy region corresponding to the extra levels in the gap yields 2.0, suggesting that these are two electrons at the occupied gap states. Such a result is very similar to that encountered in the case of an oxygen vacancy in KH_2PO_4 [24] and α-Al_2O_3 [25].

Next we will discuss the relation of oxygen vacancies to the luminescence and trap centers. Strong afterglow emissions were observed in LSO:Ce single crystals but not found in powder samples prepared by the sol–gel method in air [13]. It is probable that the single crystals contain many more oxygen vacancies than powder samples because the single crystals were prepared

under oxygen-poor conditions, in contrast to the powder samples, prepared in oxygen-rich conditions. In fact, if the samples are prepared in oxygen-rich conditions, the maximum of the oxygen chemical potential μ_O could be 0 eV; thus, the formation energies for oxygen vacancies should be elevated by 5.3 eV with respect to the calculated values for oxygen-poor conditions. Therefore, it is obvious that the formation of oxygen vacancies under oxygen-rich conditions is impossible in equilibrium conditions.

It is reasonable to make an assumption that oxygen vacancies act as traps responsible for the afterglow emission from LSO:Ce. In practice, the oxygen vacancies are more likely to exist with the 2+ charge state due to their low formation energies. For V_O^{2+}, there is no electron at the vacancy site and it could behave as an electron trap. We may give a possible model for the thermoluminescence mechanism based on assuming that V_O^{2+} as an electron trap is located in the close vicinity of the Ce^{3+} ion [26]. The trap filling can proceed by excitation of 4f electrons to 5d levels of Ce^{3+}. The electrons excited into 5d levels can be transferred to the trap center V_O^{2+}, becoming V_O^{+}, and a Ce^{4+} ion is left behind. The electron captured by V_O^{+} can be thermally released to a Ce^{4+} ion leading to a Ce^{3+} ion for the excitation state and yielding 5d 4f luminescence.

4. Conclusion

In summary, from the present calculated results, it is found that the V_{O5} have the lowest formation energies and are hence the dominant oxygen vacancies in equilibrium conditions compared with the other four oxygen vacancies belonging to the SiO_4 tetrahedron. The oxygen vacancy can induce extra states in the band gap. V_{O5} could act as an electron trap, which is responsible for the afterglow emission for LSO:Ce.

Acknowledgments

This work is supported by the Teaching and Research Award Program for Outstanding Young Teachers in Higher Education Institutions of MOE, People's Republic of China and the National Natural Science Fund of China (No. 10404028).

References

[1] Moses W W *Proc. SCINT'99 (Moscow)* p 11
[2] Cooke D W, McClellan K J, Bennett B L, Roper J M, Whittaker M T, Muenchausen R E and Sze R C 2000 *J. Appl. Phys.* **88** 7360
[3] Dorenbos P, Bos A J J and van Eijk C W E 2002 *J. Phys.: Condens. Matter* **14** L99
[4] Cooke D W, Bennett B L, Muenchausen R E, Lee J-K and Nastasi M A 2004 *J. Lumin.* **106** 125
[5] Lee J-K, Muenchausen R E, Lee J-S, Jia Q X, Nastasi M, Valdez J A, Bennett B L, Cooke D W and Lee S Y 2006 *Appl. Phys. Lett.* **89** 101905
[6] Saoudi A *et al* 1999 *IEEE Trans. Nucl. Sci.* **46** 1925
[7] van Eijk C W E 2002 *Phys. Med. Biol.* **47** R85
[8] Liu B, Shi C S, Yin M, Fu Y B, Zhang G B and Ren G H 2006 *J. Lumin.* **117** 129
[9] Dorenbos P, van Eijk C W E, Bos A J J and Melcher C L 1994 *J. Phys.: Condens. Matter* **6** 4167
[10] Cooke D W, Bennett B L, Muenchausen R E, McClellan K J and Roper J M 1999 *J. Appl. Phys.* **86** 5308
[11] Chen Y *et al* 2005 *Nucl. Instrum. Methods* A **537** 31
[12] Pidol L, Guillot-Noel O, Kahn-Harari A, Viana B, Pelenc D and Gourier D 2006 *J. Phys. Chem. Solids* **67** 643
[13] Goedecker S, Teter M and Hutter J 1996 *Phys. Rev.* B **54** 1703
[14] Gonze X, Beuken J-M, Caracas R, Detraux F, Fuchs M, Rignanese G-M, Sindic L, Verstraete M, Zerah G, Jollet F, Torrent M, Roy A, Mikami M, Ghosez P, Raty J-Y and Allan D C 2002 *Comput. Mater. Sci.* **25** 478
[15] Troullier N and Martins J L 1991 *Phys. Rev.* B **43** 1993

[16] Monkhorst H J and Pack J D 1976 *Phys. Rev.* B **13** 5188
[17] Press W H, Flannery B P, Teukolsky S A and Vetterling W T 1989 *Numerical Recipes. The Art of Scientific Computing (FORTRAN Version)* (Cambridge: Cambridge University Press)
[18] Zhang S B and Northrup J E 1991 *Phys. Rev. Lett.* **67** 2339
[19] Laks D B, Van de Walle C G, Neumark G F, Blöchl P E and Pantelides S T 1992 *Phys. Rev.* B **45** 10965
[20] Zhang S B, Wei S H, Zunger A and Katayama-Yoshida H 1998 *Phys. Rev.* B **57** 9642
[21] Jacobsohn L G, Bennett B L, Lee J-K, Muenchausen R E, Smith J F, Uberuaga B P and Cooke D W 2007 *J. Lumin.* **124** 173
[22] Anderson P W 1975 *Phys. Rev. Lett.* **34** 953
[23] Makov G and Payne M C 1995 *Phys. Rev.* B **51** 4014
[24] Liu C S, Hou C J, Kioussis N, Demos S G and Radousky H B 2005 *Phys. Rev.* B **72** 134110
[25] Matsunaga K, Tanaka T, Yamamoto T and Ikuhara Y 2003 *Phys. Rev.* B **68** 085110
[26] Dorenbos P, van Eijk C W E, Bos A J J and Melcher C L 1994 *J. Phys.: Condens. Matter* **6** 4167